Hindawi
International Journal of Photoenergy
Volume 2023, Article ID 5749756, 15 pages
https://doi.org/10.1155/2023/5749756

Research Article

Energy Management System for Smart Grid in the Presence of Energy Storage and Photovoltaic Systems

Alireza Kermani,[1] Amir Mahdi Jamshidi,[1] Zahra Mahdavi,[1] Amir ali Dashtaki,[2] Mohammad Zand,[1] Morteza Azimi Nasab,[1] Tina Samavat,[1] P. Sanjeevikumar,[1] and Baseem Khan[3,4]

[1]*Department of Electrical Engineering, IT and Cybernetic, University of South-Eastern Norway, Kjølnes Ring 56, 3918 Porsgrunn, Norway*
[2]*Great Tehran Electric Distribution Company, Tehran, Iran*
[3]*Department of Electrical and Computer Engineering, Hawassa University, Hawassa, Ethiopia*
[4]*Department of Electrical and Electronic Engineering Technology, Faculty of Engineering and the Built Environment, University of Johannesburg, South Africa*

Correspondence should be addressed to Baseem Khan; baseem_khan04@yahoo.com

Received 25 June 2022; Revised 14 April 2023; Accepted 7 July 2023; Published 21 November 2023

Academic Editor: Alberto Álvarez-Gallegos

Today, the desire to use renewable energy as a source of clean and available energy in the grid has increased. Due to the unpredictable behavior of renewable resources, it is necessary to use energy storage resources in the microgrid structure. The power generation source and the storage source in microgrids should be selected in such a way that it has the ability to respond to the maximum demand in the state connected to the grid and operate independently. In this article, the optimal capacity and economic performance of a microgrid based on photovoltaic and battery system have been investigated. In this way, first, using the iterative optimization method, the optimal microgrid capacity has been obtained. Then, the dynamic planning method has been used for optimal microgrid energy management. The simulation results show the accuracy and efficiency of the proposed solutions. The proposed controller, while automatically and dynamically adapting to the solar cell output changes, is capable of responding to external requests, such as price signals or satisfying power system constraints or operator requests. In addition, the results indicate that by using the proposed energy management system, the microgrid system can regain stability during one to two cycles, during the occurrence of PV system radiation changes as well as ESS charge changes. And also, according to the ESS charge changes, the voltage changes should be within the defined permissible range between 0.95 and 1.05 pu, which is the result of the unique efficiency of the proposed energy management system.

1. Introduction

The concerns of the world community regarding the environment have caused the use of scattered products that use new energy production sources to increase rapidly. But the nature of most new energies is variable and unpredictable, which has become an obstacle for the wider use of new energies. To solve this problem, energy storage sources are used [1–3], which solve the unpredictable and variable nature of new energies. Electrical microgrids consisting of distributed production sources are the main elements of the future smart grid, which will play an important role in reaching the aforementioned goals. The microgrids created on the distribution side provide the conditions for the operation of DG resources. These resources include new technologies such as diesel generators, microturbines, and fuel cells, which, along with photovoltaic systems and wind turbines, will be responsible for feeding part of the consumer demand on the distribution side [4]. Coordination between these sources with energy storage elements and controlled loads (such as air conditioning equipment) will be one of the challenges facing electric microgrids [5, 6]. Depending on the location and conditions of electrical networks, different scenarios have been defined in the operation of electrical microgrids. Microgrids are mostly operated when connected to the upstream grid, in which case, the needs of consumers are met by the energy received from the main grid and the energy produced by their own internal resources. But in some situations (such as supplying loads to remote areas or during maintenance of a part of the network), these microgrids can also work in separate mode. In this case, the supply of the entire load is the responsibility of domestic sources [7].

With the advances made in the technology of energy storage elements, the use of these equipment's will determine the achievement of a flexible network. The presence of storage elements enables the operator to operate the network with higher reliability and with lower production costs. In reference [8], the authors have presented a solution for the optimal use of the microgrid, based on which, the cost of the microgrid is significantly reduced by storing energy in low load hours and selling it in peak load hours. The algorithm used in solving the optimization problem was PSO.

In reference [9], a similar work has been done by minimizing the cost of microgrid operation with the help of linear programming algorithm. Another strategy based on the participation of wind turbine and energy storage elements has been proposed in [10], which also considered the random nature of wind turbine output. Also, in this reference, the researchers have presented an intelligent energy management system (SEMS), whose task is to create coordination between power forecasting, energy storage, and energy exchange with the main grid, which leads to an optimal production planning in the period of time. Short term (next 24 hours) leads. Another important point in using microgrids is how to interact with the main grid. Considering that microgrids have the ability to connect with the main grid, they can receive energy from the grid in case of shortage. Therefore, it is necessary to receive information about the status of the main network every hour in order to use them in the operation of the microgrid.

In order to optimize energy management in microgrids, algorithms have been proposed in the literature so far. Law-based optimal energy management in an island microgrid is described in [11, 12]. In [13], energy management is performed in an island microgrid consisting of PV and WT as the main sources and fuel cell as the backup system. The operation of this system depends on the developed rules. Despite observing all the limitations under the optimizations performed in these two references, the results are not comprehensive. In reference [14], microgrid has a combined topology, including PV and fuel cell. The presence of fuel cells is less due to the improvement of power quality in voltage drop. Among the objectives of this reference are to reduce the size of PV, reduce costs, increase reliability, and create a compact structure. Reference [15] deals with optimal management in a hybrid microgrid, including WT battery. This reference assumes that information such as production volume, load demand, and instantaneous price is available. In order to eliminate the dilemma between long-term planning of storage devices for economic reasons and short-term planning of WT production and load demands, two-scale dynamic planning has been used. The simulation results show a reduction in energy costs under the two-scale method compared to the single-scale method. In [16, 17], fuzzy logic estimates rules in improving the law-based method. The proposed method in [18] consists of two steps: one is to determine the behavior of the energy management system by fuzzy logic, and the other is to determine the appropriate parameters for the fuzzy controller. The general purpose of the proposed method is to minimize the fuel consumption of parallel vehicles.

In [19], the optimal energy management of a microgrid is performed with the help of game theory and multiobjective optimization. In this reference, the operating cost and the level of pollution are considered as the objective function. Electronic power converters play a key role in controlling the flow of energy in a microgrid. For this purpose, the measured information is used in the control and monitoring of distributed generation sources. In communicating between a microgrid with other system components such as the distribution system operator, central control is used, and in controlling several microgrids in a feeder, the distributed management system is used. These control methods can be implemented in the form of a hierarchical controller, including three levels.

Among other control methods, centralized control can be mentioned. The basic principles of this method are to determine the average current. In fact, by considering the total load current, the current reference of each power generation unit will be determined [20]. Then, a current error is obtained and sent to the current control loop, and the command signal of the switches is generated. Other methods in this field include the follower method [21] and drop control [22]. Reference [23] uses a PV-battery composite structure in a microgrid for home use. Reason battery and diesel generators have been used as a backup to solve the problems of renewable sources.

In reference [24, 25], the dynamic programming method is used to manage the optimal energy for the microgrid based on the PV battery connected to the grid. The purpose of this method is to minimize the energy received from the grid. Problem constraints also include balancing each resource's production/consumption and capacity. The results show that the dynamic planning method performs better than the law-based method. Reference [26–30] presents a two-tier hierarchical control strategy for a flexible inverter-based microgrid. This inverter can operate in either grid or island mode. The simulation results show that the acceptable microgrid performance under study [31–38] presents a hierarchical control strategy for parallel power supply inverters in an island microgrid. The proposed control method consists of drop control, virtual impedance control, compound voltage control, and sliding mode control.

Therefore, integrating the power grid with the PV system is one of the topics worth researching. Also, the battery can be used as a lever to increase the penetration of the PV system. Despite the advantages that this structure can provide

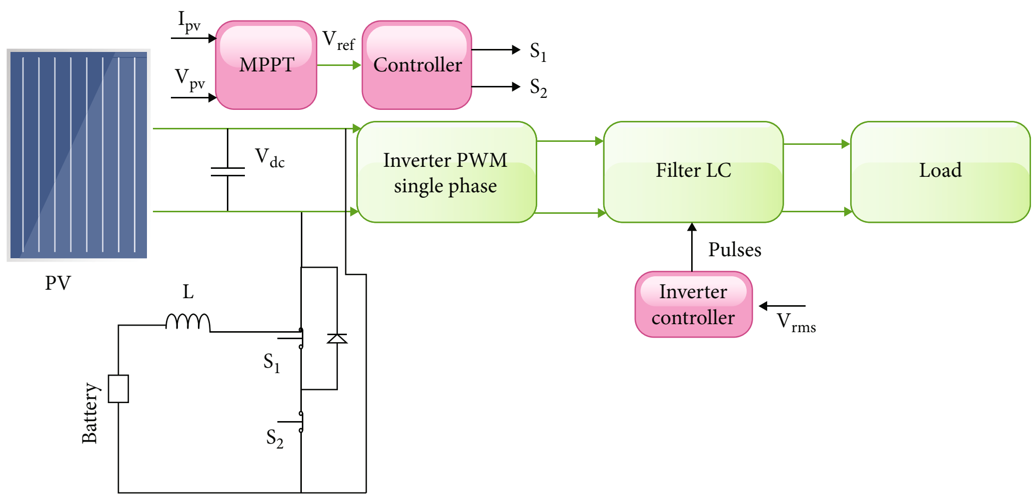

Figure 1: Combined power generation system.

for setting up an intelligent network, it is always associated with challenges that affect the microgrid's performance. The optimal estimation and economic performance of a microgrid, along with other performance characteristics such as high reliability, require an accurate and efficient control strategy.

The main purpose of this paper is optimal energy management in a microgrid based on PV and battery usage. Among other goals that will be achieved in this regard, we can mention the optimization of microgrid size and optimal power exchange between the power network and microgrid.

2. Energy Management Optimization for a Grid Connected to the Grid

The microgrid structure under study in the network connection mode includes a power network, solar panel, and battery. The power grid directly meets the microgrid load requirement through the AC bus. When the power output of the panel system is insufficient, the power shortage is compensated by the battery or power grid. In contrast, the excess power produced by PV will first fully charge the battery, and then, the rest of the power will be injected into the power grid. Therefore, having an energy management system in order to schedule resources to achieve the objective function is essential. Figure 1 presents the model of combined power generation system.

2.1. Cost Function. The objective function considered in Equation (1) minimizes the final CF value. The CF parameter includes received cost (CR) and paid cost (CP). CR value is defined negatively, and CP value is defined as positive. That is,

$$\min\ (\mathrm{CF}) = \min\left(\sum_{t_0}^{T} \mathrm{CR}(t) + \mathrm{CP}(t)\right). \tag{1}$$

The amount of CR is considered a benefit obtained from selling excess power to the power grid. The value of this parameter is in the form

$$\mathrm{CR}(t) = P_{\mathrm{grid}}(t).\mathrm{FIT}(t).t. \tag{2}$$

In the above relation, the parameters P_{grid} and FIT are the power injected into the network and the sales tariff, respectively, considered by the microgrid. The amount of CP includes the cost of electricity purchased from the power grid and the cost of replacing the battery. The following equation can also calculate the value of this parameter:

$$\mathrm{CP}(t) = \left(P_{\mathrm{grid}}(t).(t).\mathrm{Eg}_P(t).t + \mathrm{Br}_C(t)\right). \tag{3}$$

In the above relation, the parameters P_{grid}, Eg_P, and Br_C are the power purchased from the network (with a positive value), the electricity tariff, and the battery replacement cost, respectively. Therefore, the objective function of the problem under study is written as follows:

$$\min\ (\mathrm{CF}) = \min\left(\sum_{t_0}^{T} P_{\mathrm{grid}}(t).\mathrm{FIT}.t + P_{\mathrm{grid}}(t).t.\mathrm{Eg}_P(t).t + \mathrm{Bi}_c\,\frac{Z.(\mathrm{SOC}_{xi}(t-\Delta t) - \mathrm{SOC}_{xi}(t))}{1-\mathrm{SOH}_{\min}}\right). \tag{4}$$

In the above relation, Z is considered equal to 0.0003, and Bi_c is the investment cost of the battery. The parameters P_{grid} and Eg_P are the power purchased from the network and the electricity cost, respectively.

2.2. Limitations. In this section, the limitations of the proposed method are mentioned.

(i) Power adjustment limit

Output power of the battery

$$P_L(t) = P_{\mathrm{PV}}(t) + P_B(t) + P_{\mathrm{grid}}(t), \tag{5}$$

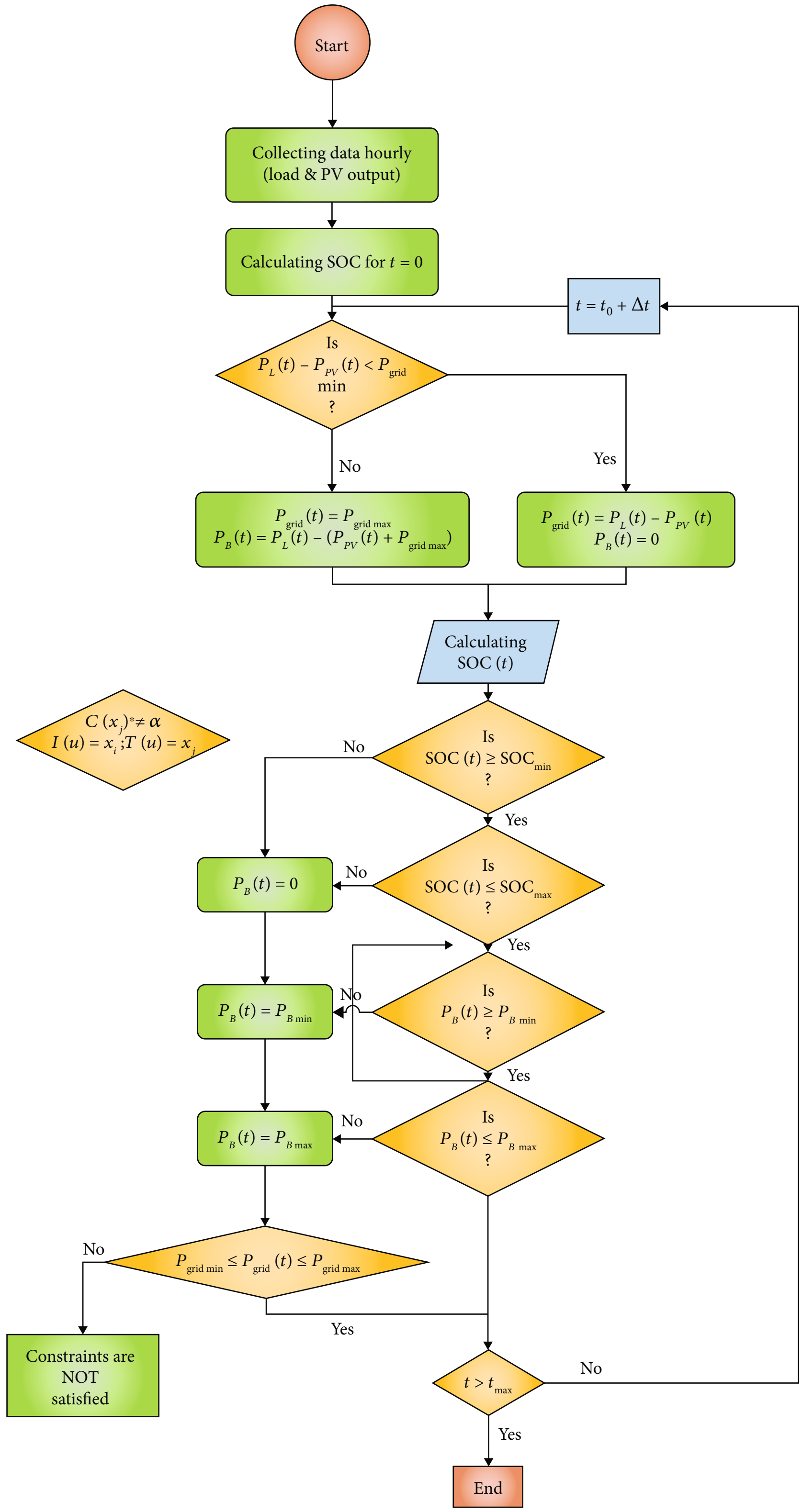

Figure 2: Law-based energy management flowchart.

$$\text{PBmin} \leq \text{PB}(t) \leq \text{PBmax}. \tag{6}$$

(ii) Battery SOC limit

$$\Delta\text{SOC}_{\text{min}} \leq \Delta\text{SOC}(t) \leq \Delta\text{SOC}_{\text{max}}, \tag{7}$$

$$\text{SOC}_{\text{min}} \leq \text{SOC}(t) \leq \text{SOC}_{\text{max}}. \tag{8}$$

(iii) Battery life time limit

$$\text{SOH}(t) \geq \Delta\text{SOH}_{\text{min}}. \tag{9}$$

(iv) Network power limit

$$P_{\text{grid min}} \leq P_{\text{grid}}(t) \leq P_{\text{grid max}}. \tag{10}$$

In order to minimize the power received from the power grid, the value $P_{\text{grid max}}$ is limited as follows:

$$\begin{aligned} 0 \leq P_{\text{grid max}} &\leq P_{\text{peak load}}, \\ P_{\text{grid min}} &= -P_{\text{grid max}}. \end{aligned} \tag{11}$$

In this paper, the value of $P_{\text{peak load}}$ is considered equal to 50 kW.

2.3. Rule-Based Energy Management Strategy. This section proposes a "constraint" management strategy based on predefined rules for network-connected microgrids.

Rule-based energy management guidelines have the following main rules:

(i) The PV system primarily provides loads

(ii) The battery is discharged only when the PV power and network are insufficient

(iii) The battery is charged as soon as the first available source is found

Rule-based energy management has the limitations mentioned in Equations (5), (6), (7), and (10).

The approach of this method is as follows:

(i) Power grid power is determined as a PV and load power function

(ii) Battery capacity is also calculated according to the assigned relationships

(iii) The obtained values are confirmed according to the considered restrictions

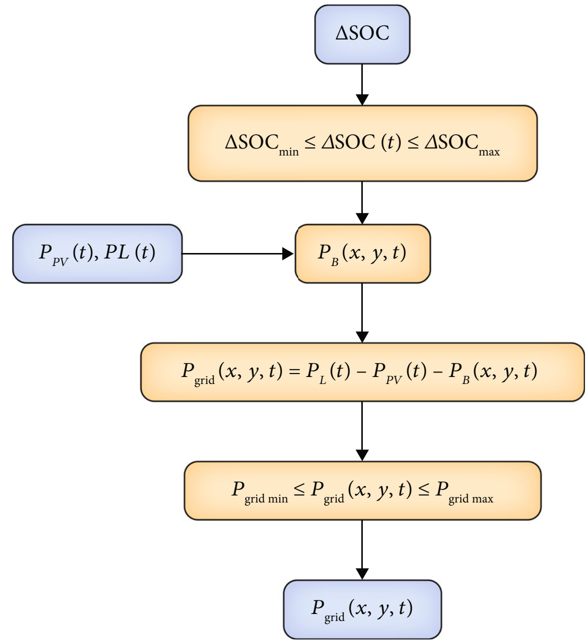

Figure 3: P_B and P_{grid} calculation process.

(iv) The maximum power delivered from the power grid is the same as the optimal value obtained by the DP method

Figure 2 presents the law-based energy management flowchart.

2.4. Application of the Bellman Algorithm in Microgrid Energy Management Connected to the Grid. Battery power (PB) is obtained by changing the SOC (ΔSOC). Network power is obtained by specifying P_B, given that P_L and P_{PV} values are also available. The value obtained must be true under the conditions considered.

Figure 3 presents the P_B and P_{grid} calculation process.

Given the initial vector $P_{\text{grid max}}$ as

$$P_{\text{grid max}} = \{P_{\text{grid}\,i\ \text{max}}\}, i = 1, \cdots, k, \tag{12}$$

for each element of this vector, the Bellman algorithm finds the minimum value of CF_i.

Assuming that

$$A_i = \text{argmin}\,\text{CF}_i, \tag{13}$$

after several times of analysis, the optimal energy management of a grid connected to the grid is defined as the minimum value of vector A:

$$\min(A), A = \{A_i\}. \tag{14}$$

The optimal capacity of the PV-battery system connected to the network has been investigated in this section. The radiation intensities and the load profiles considered in this regard are shown in Figures 4 and 5, respectively.

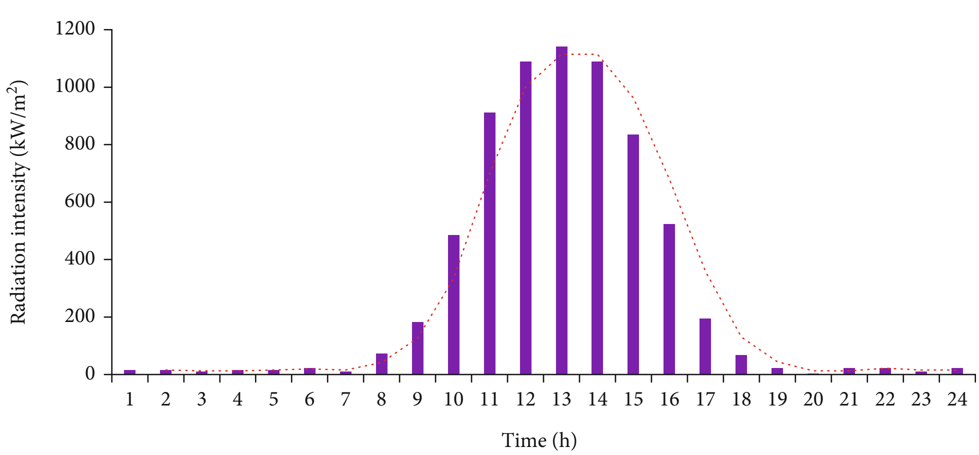

Figure 4: Radiation intensity curve.

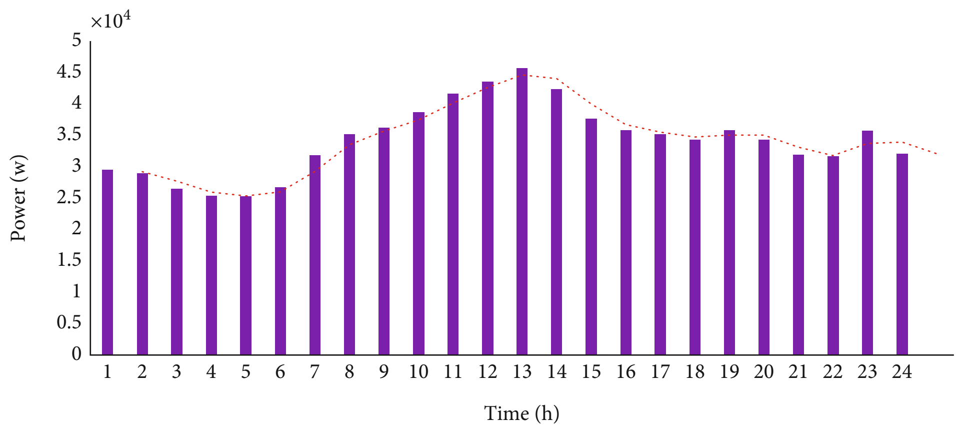

Figure 5: Load variation curve.

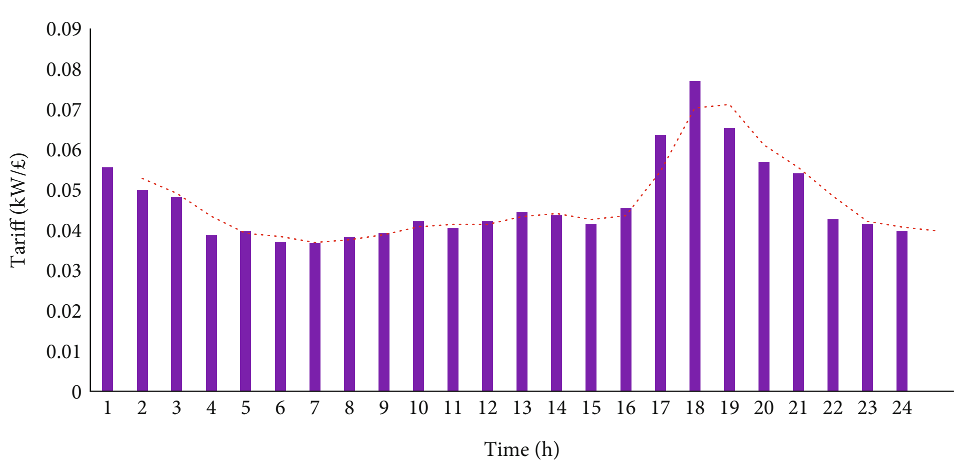

Figure 6: Electricity dissipation.

Also, the electricity tariff and flowchart of the proposed method are shown in Figures 6 and 7, respectively. This algorithm first receives data such as radiation intensity, temperature, and load for different hours. Then, it calculates different values of N_{pv} and C_B (battery capacity). Thus, in each iteration, ACS is calculated according to the capacity of PV and battery. These calculations are continued until each N_{pv} and C_B parameter reaches its maximum value.

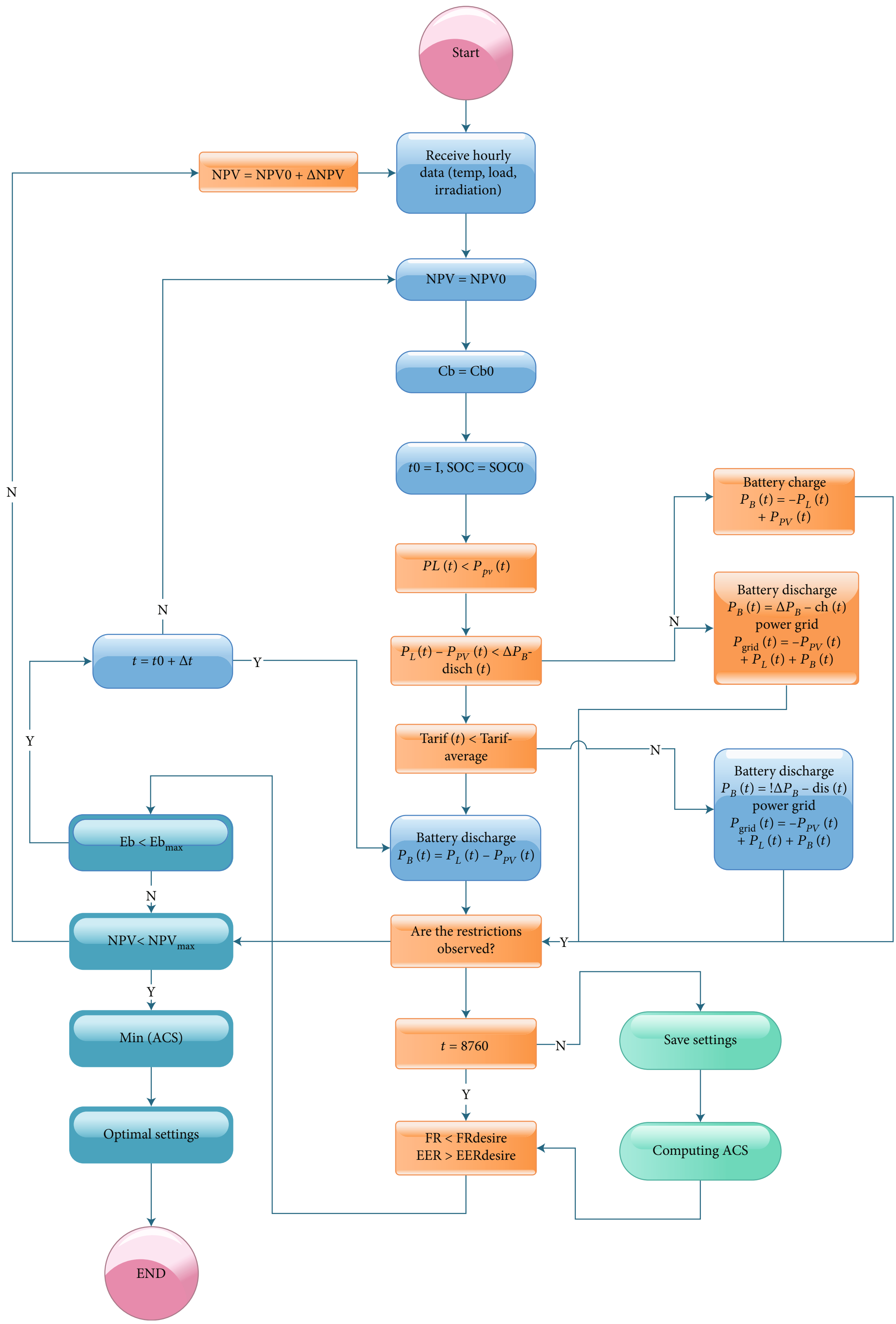

Figure 7: Flowchart for calculating the optimal microgrid capacity.

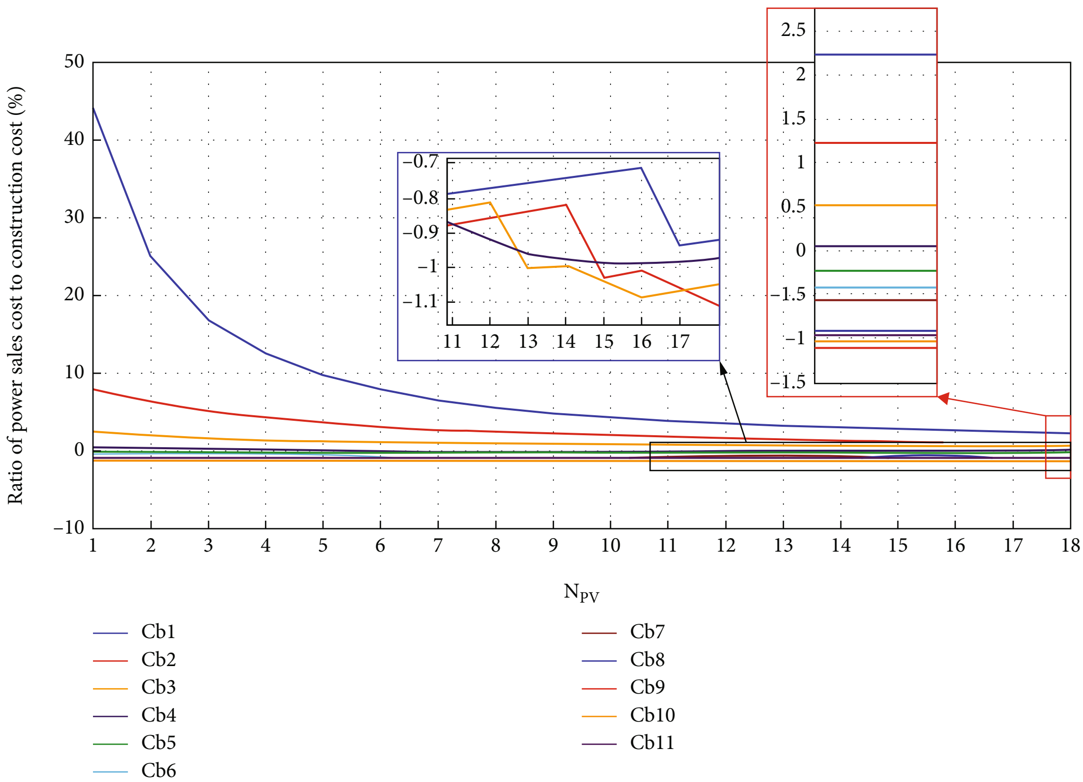

Figure 8: Percentage of profit to microgrid cost ratio curve under N_{pv} changes and different battery capacities.

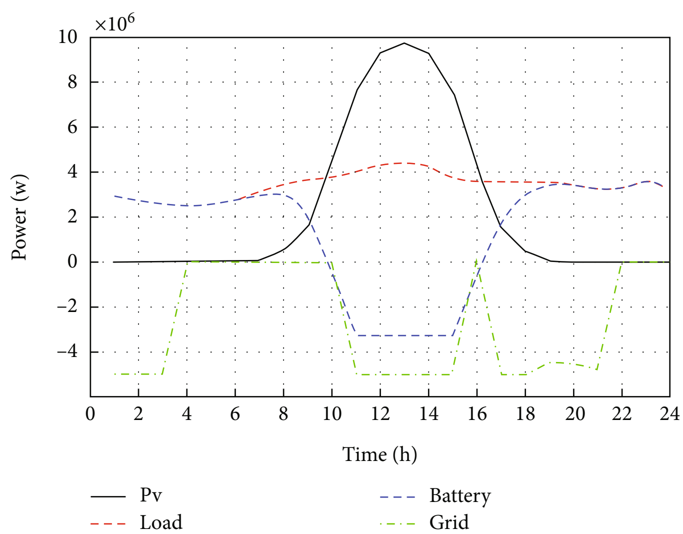

Figure 9: Load, PV, battery, and network change curves under optimal microgrid capacity.

Finally, the values of N_{pv} and C_B for which the minimum ACS is obtained are extracted. This flowchart is designed to calculate the optimal microgrid capacity during a year. Since one-year data are unavailable, the optimal microgrid size is obtained here with only one summer day in mind. In the ACS calculation, the FR value is 1 (i.e., the microgrid is supplied by RES only), and the EER is 0.01 for each day.

The flowchart shown in the figure above is coded in MATLAB software. The maximum values of N_{pv} and C_B are 18 and 110 kWh, respectively. In each step, the amount of P_{pv} increases by 1 unit (during 18 steps) and the amount of C_B by 10 kW (during 11 steps). In order to examine the financial benefits more closely, the amount of profit from the sale of surplus power has also been calculated for different amounts of ACS. Since in this article, the power signal sold to the grid is considered negative, and the power signal received from the grid is considered positive; in case the profit from the power exchange with the grid reaches its maximum, the final cost is negative higher. This is well illustrated in Figure 8. Thus, at $N_{pv} = 18$, the optimal battery capacity for step 9 is 90 kW. However, for $N_{pv} = 16$, the optimal battery capacity value is 100 kW.

The power change curve is obtained during one day according to the optimal number of N_{pv} and C_B. These curves are shown in Figure 9. As shown in this figure, the charge is fed through the battery as long as the P_{pv} is zero. Here, a positive value of battery power is a discharge of the battery, and a negative value is a charge of the battery. Meanwhile, if the electricity tariff exceeds the average overnight tariff, part of the battery capacity will be sold to the network. When PV generates power, the required power of the load is fully supplied, and the excess PV power is sold to the network or used to charge the battery. At the end of the day and as the PV power decreases, the battery responds to the load again and sells electricity to the grid at certain times. As it is known, the battery's capacity is determined in such a way that no power is received from the power grid day and night.

3. Optimal Microgrid Management

This section discusses the optimal energy management of a microgrid in network connection mode. The curve related to changes in radiation intensity and the load is considered as in the previous section. Table 1 shows the values of the parameters considered in the simulation. In this section, the Bellman algorithm determines the minimum value of the objective function described in Equation (15). In this equation, $\mathrm{FIT}(t)$ is the tariffs for the sale of surplus microgrid power, $\mathrm{Eg}_p(t)$ is the tariffs for electricity of the network, and Br_C is the cost of replacing the battery.

$$\mathrm{CF} = \sum_{1}^{T}\left(\left(P_{\mathrm{grid}}(t).\mathrm{FIT}(t).t\right) + \left(P_{\mathrm{grid}}(t).\mathrm{Eg}_P(t).t + \mathrm{Br}_C(t)\right)\right). \tag{15}$$

The coding of the Bellman algorithm is also done in MATLAB software. Figure 10 shows an example of the output of the implemented code for three hours. In this figure, each row (except the first row: node 1) represents one hour of the day. Nodes in a row also represent the number of states intended to change the SOC. For example, in the figure below, the SOC can take three values. Accordingly, the nodes in columns (i.e., 2 and 5) have a minimum value of SOC, the nodes in the right column (i.e., 4 and 7) have a maximum value of SOC, and the nodes in the middle column (3 and 6) have a value between minimum and maximum.

Nodes 1 and 8 are equal to the initial and final SOC, respectively. As it turns out, each branch has a value or the same weight calculated based on the same values of the path's cost between the initial and final SOC. Since the number of nodes in this figure is relatively small, achieving the optimal path at a low cost is shown in Figure 11. In this figure, there are 92 nodes and 1155 branches. To achieve a better display and prevent the shape from getting crowded, the weight values of the branches are not shown in this figure. The optimal path in this figure is shown in green. It is clear that the Bellman algorithm selects different values of SOC at different times during this path. As mentioned earlier, the logic of selecting SOCs is also according to the objective function and the terms and conditions.

According to the information in Table 1, there will be 15 nodes per hour (except 24 hours). The total number of

Table 1: Simulation parameters.

Measure	Value	Parameter
Hour	24	Simulation time (T)
Hour	1	Time step (Δt)
Percentage	50	Initial SOC
Percentage	80	Final SOC
Percentage	20	Minimum SOC (per hour)
Percentage	90	Maximum SOC (per hour)
Percentage	5	Step time for each SOC
Percentage	70	SOH min
kW	70	Maximum exchange power with the network

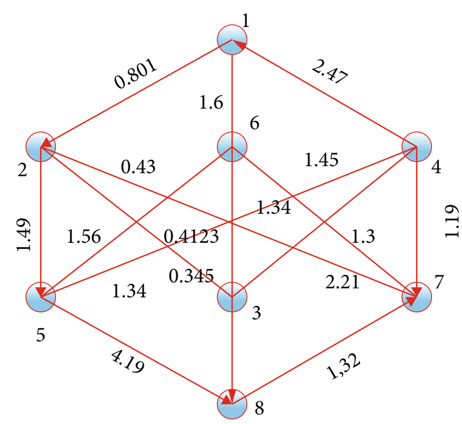

Figure 10: Implementation of the Bellman algorithm for 3 hours (including 8 nodes and 15 branches).

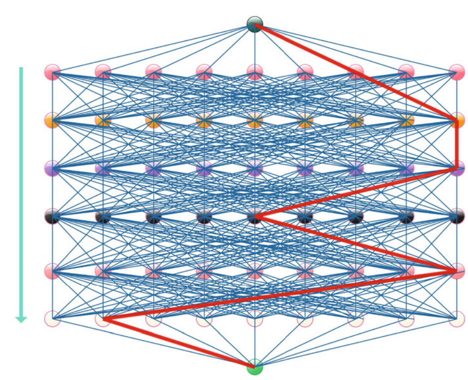

Figure 11: Demonstration of the optimal path in the Bellman algorithm for 7 hours (with 92 nodes and 1155 branches).

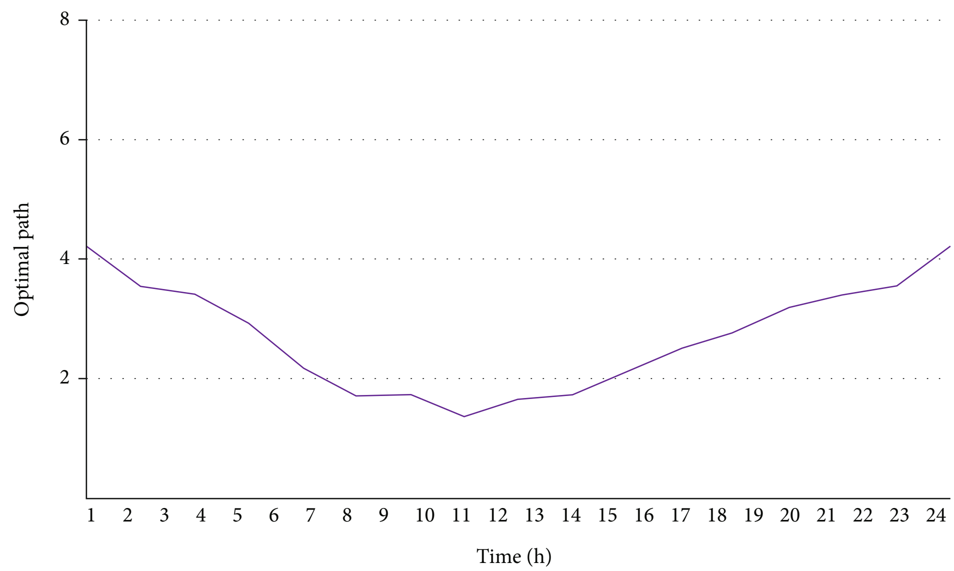

FIGURE 12: Demonstration of the optimal path in the Bellman algorithm for 24 hours.

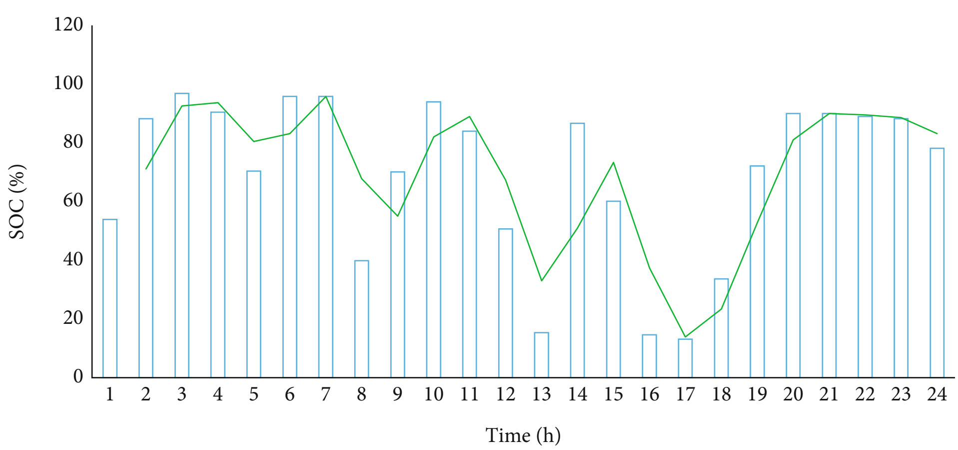

FIGURE 13: Optimal SOC changes.

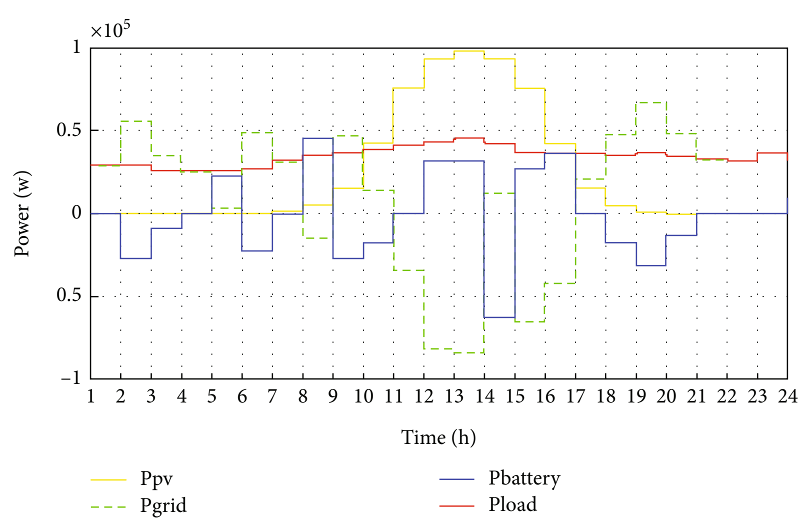

FIGURE 14: Power change curve of microgrid components under optimal management.

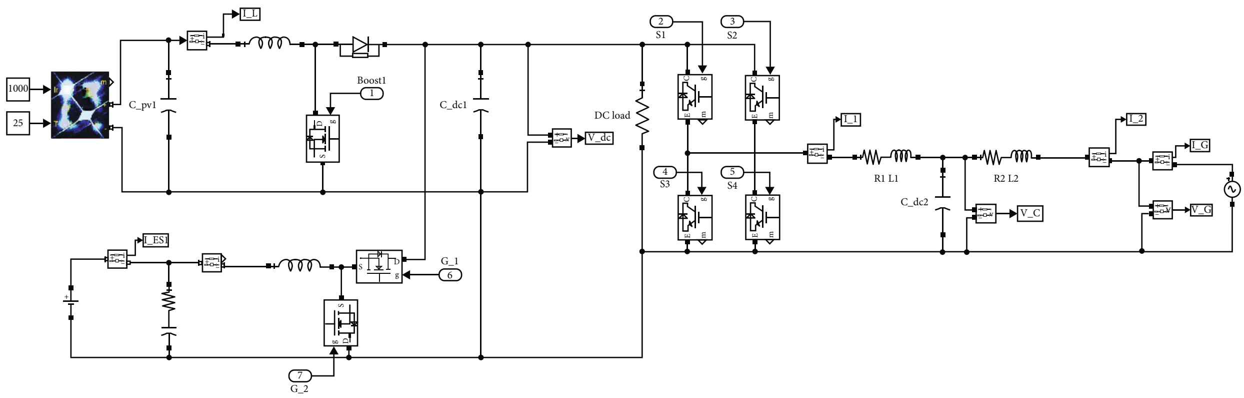

Figure 15: Overview of PV microgrid battery connected to mains.

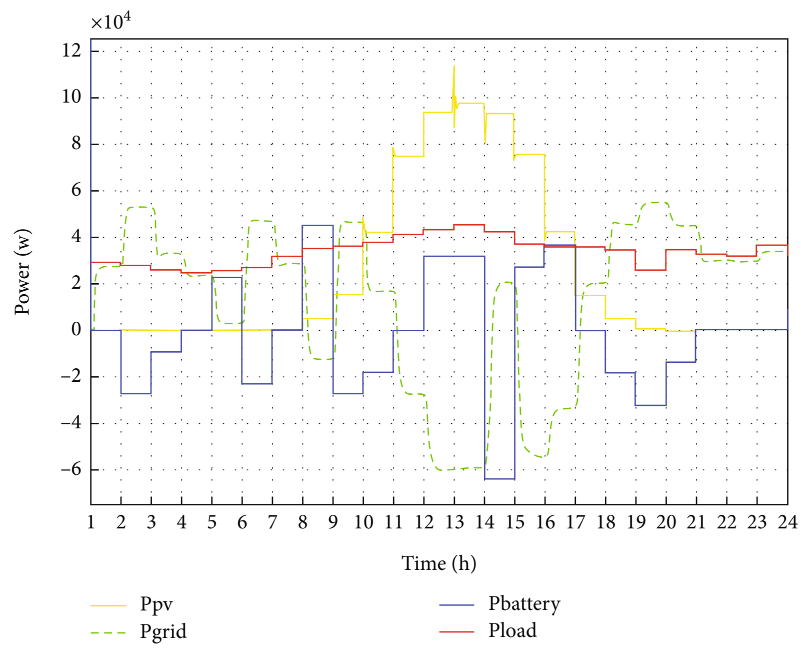

Figure 16: Curve of power changes of microgrid components under optimal management.

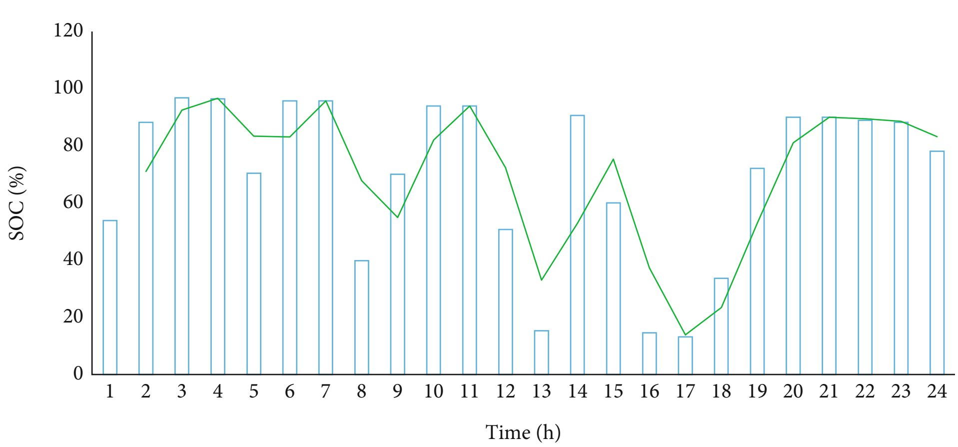

Figure 17: SOC changes under optimal microgrid performance.

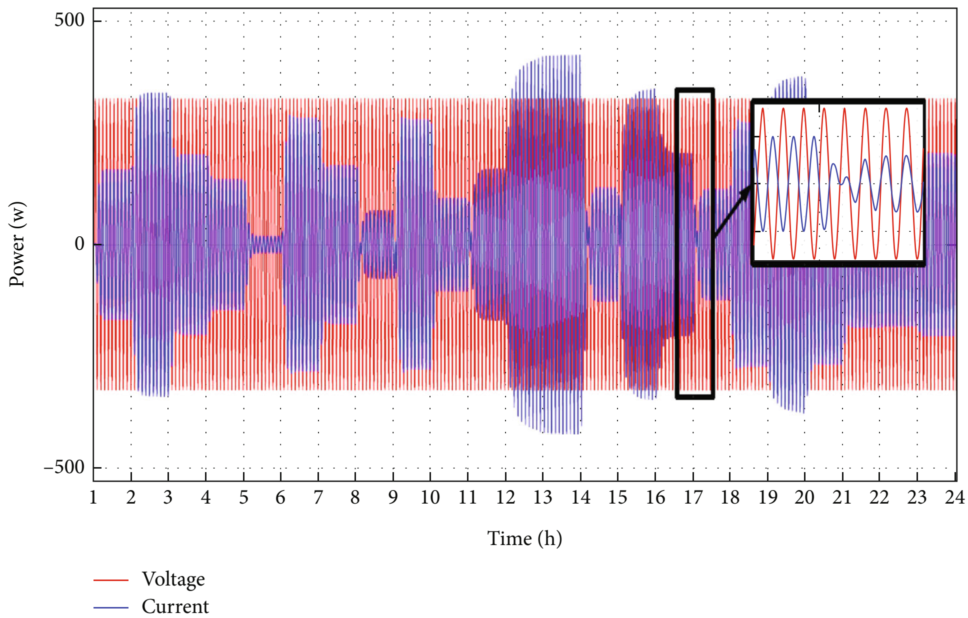

Figure 18: Voltage and current toward the power grid.

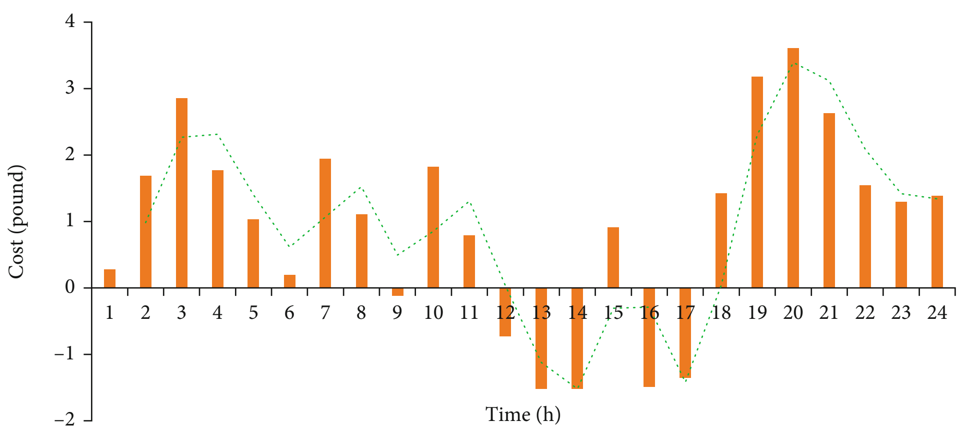

Figure 19: Microgrid electricity cost curve.

nodes will be 347, and the total number of branches will be 4980. The plot command in MATLAB will not be able to draw graphs with more than 100 nodes. Thus, in drawing such graphs, changes such as nonautomatic labeling of nodes reduce the size of nodes and branches are applied to make the result of the work visible. However, the result will not give the reader an understandable figure such as Figures 10 and 11. For example, the processing result of the Bellman algorithm for the case where the number of nodes is 347 and the number of branches is 4980 is shown in Figure 12.

Although the resulting figure is incomprehensible, the results of Bellman's analysis can be extracted manually from the workspace. Figure 13 shows the optimal SOC changes under the capacities obtained in the previous section.

According to the SOC curve in the figure above, first, the amount of charge and discharge power of the battery is determined; then, according to the values of PV power and load consumption, the amount of power exchanged with the power grid will be calculated. Thus, Figure 14 shows the changes in PV output power, load consumption power, battery charge/discharge exchange power, and power exchange with the power network under coding. In this figure, the positive values of power grid power and battery power indicate the power delivered from the grid and the discharge power of the battery, respectively. The negative values of these two parameters also indicate the injection power and battery charging power, respectively.

This section simulates a microgrid sample based on a PV battery with optimal capacity and performance under optimal management. An overview of the simulation in MATLAB Simulink is shown in Figure 15. In this simulation, a DC-DC boost converter is used to connect the PV to the DC link, a two-way DC-DC converter is used to

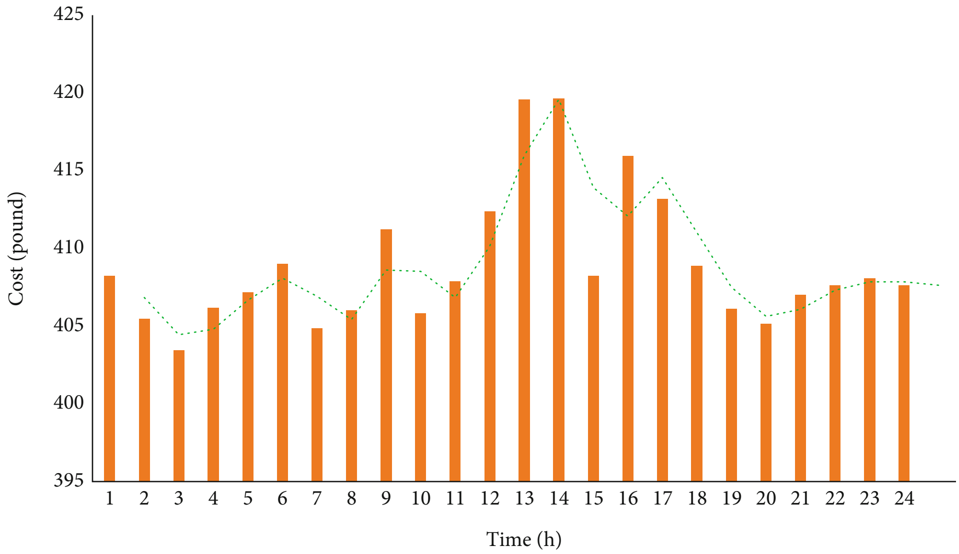

Figure 20: DC link voltage.

Table 2: Comparison of the proposed energy management method with reference [15].

Optimization technologies: rule-based algorithm	Objective	Decision variable	Application strategy	Target
Reference [15]	Peak shaving	Power flow	Control	Grid-connected microgrid of a sport centre facility
	Economic dispatching	—	—	—
Proposed method	Self-consumption	Power flow	Control sizing	Building with PV system
	Peak shaving	Capacity	—	—
	Price arbitrage			
	Npv	Power flow	—	—

connect the battery to the DC link, and an inverter is used as the interface between the DC link and the power grid. A variable DC load is also connected to the DC link. The load curve changes according to what is considered in the coding space (Figure 14).

The power exchange curve between the various components in the microgrid under study is shown in Figure 16. These results are obtained from simulation and under optimal microgrid management.

The power exchanges shown in the figure above are based on the optimal SOC reference in Figure 14:

(1) The SOC difference is calculated for two consecutive hours based on the SOC curve

(2) The battery exchange capacity is determined to meet the SOC difference obtained

(3) The battery power reference is divided by its voltage into the current reference

PV boost converter also produces the most available power due to the radiation intensity. Also, if there is excess power, the inverter injects it into the network. Conversely, in the event of a shortage, it will receive the power it needs from the grid. As a result, the SOC of the microgrid battery will change, as shown in Figure 17.

The voltage and current change curves of the power grid side are shown in Figure 18.

As shown in the figure above, the current and voltage on the grid side have no phase difference. Also, the grid current is stabilized during one to two cycles, according to the intended situation. The cost/receipt of the microgrid to the network is calculated by multiplying the purchase/sale tariff by the consumption/sales capacity. Accordingly, the microgrid cost curve is shown in Figure 19. The average value of this curve is 0.9221 pounds. This figure indicates that the microgrid under study should pay the same amount to the network operator for its overnight consumption. Since the final SOC of the battery is 80% and the initial SOC is 50%, the positive result of the charges was not unexpected.

The DC link voltage changes are shown in Figure 20. This figure shows that the DC link voltage varies under different conditions around the reference value (i.e., 410 volts). Only in one case, at the beginning of the 12th hour, when the battery power starts to discharge at the highest rate and the PV output power is at its maximum, the DC link's voltage increases. This voltage increase can be adjusted by resetting the coefficients of the control system. However, since the time step for change in this paper is 0.2 seconds, achieving a stable state quickly in this short period is not easy.

As it is clear in Table 2, the proposed method has been compared with reference [15]. It is found that reference [15] only performed a control evaluation by the energy management system, while the proposed method of energy management in this article has been able to simultaneously control and size the microgrid in the presence of PV and ESS.

4. Conclusion

In this article, determining the optimal capacity, control, and energy management strategy for a microgrid based on PV and battery has been researched and developed. The models of microgrid elements have been developed in line with the different goals of this article. The correctness and accuracy of the developed models have been investigated by the simulation results. Finally, an iteration-based method has been used in order to find the optimal capacity of the microgrid including PV and battery in the state of connection to the grid. The optimal structure is not only effective in achieving technical conditions and reducing energy costs. The results indicate that the proposed method is aimed at optimal energy management in grid connection mode, minimization of microgrid power exchange with power grid, reduction of energy cost, and increase of PV efficiency.

Abbreviations

PLL: Phase-locked loop
RB: Rule-based
CR: Cash received
SS: Single-source
CC: Cash pay
DP: Dynamic programming
EER: Excess energy ratio
REF: Renewable energy fractions
ACS: Annual cost of the system
ACC: Annual capital cost
ARC: Annual replacement cost
AOM: Annual operation maintenance
ASC: Annual selling cost
HC: Hierarchical control
GT: Game theory
SOC: State of charge
MPPT: Maximum power point tracking
PCI: Parallel-connected inverters
ESS: Energy storage systems
BMS: Battery management system
NLP: Nonlinear programming problem
PV: Photovoltaic system
BESS: Battery energy storage systems
DERs: Distributed energy resources
LV: Low voltage
RES: Renewable energy sources
ML: Hysteresis current controller
SMC: Sliding mode control
PRC: Proportional resonant controller
PIC: Proportional integral controller
IPV: Fuzzy logic control
MG: Microgrid
EER: Excess energy ratio
VI: Virtual impedance
EMS: Energy management strategy
LIB: Lithium-ion battery.

Data Availability

Data will be available on request. For the data-related queries, kindly contact Baseem Khan (Baseem_khan04@yahoo.com).

Conflicts of Interest

There is no conflict of interest of any author in any form.

References

[1] M. Zand, M. A. Nasab, A. Hatami, M. Kargar, and H. R. Chamorro, "Using adaptive fuzzy logic for intelligent energy management in hybrid vehicles," in *2020 28th Iranian Conference on Electrical Engineering (ICEE)*, Tabriz, Iran, 2020.

[2] H. Ahmadi-Nezamabad, A. Alizadeh, M. Vosoogh, and S. Nojavan, "Multi-objective optimization based robust scheduling of electric vehicles aggregator," *Sustainable Cities and Society*, vol. 47, article 101494, 2019.

[3] M. Zand, M. A. Nasab, P. Sanjeevikumar, P. K. Maroti, and J. B. Holm-Nielsen, "Energy management strategy for solid-state transformer-based solar charging station for electric vehicles in smart grids," *IET Renewable Power Generation*, vol. 14, no. 18, pp. 3843–3852, 2020.

[4] O. H. Milani, S. Motamedi, S. Sharifian, and M. Nazari-Heris, "Intelligent service selection in a multi-dimensional environment of cloud providers for Internet of Things stream data through cloudlets," *Energies*, vol. 14, no. 24, p. 8601, 2021.

[5] T. Nguyen, A. Parekh, A. E. Cetin, and B. Prasad, "0537 Incident Hypertension prediction in obstructive sleep apnea using machine learning," *Sleep*, vol. 46, Supplement_1, pp. A236–A237, 2023.

[6] C. Xue, J. Wang, and Y. Li, "Model predictive control for grid-tied multi-port system with integrated PV and battery storage," *IEEE Transactions on Smart Grid*, vol. 13, no. 6, 2022.

[7] M. H. Elkholy, H. Metwally, M. A. Farahat, T. Senjyu, and M. Elsayed Lotfy, "Smart centralized energy management system for autonomous microgrid using FPGA," *Applied Energy*, vol. 317, article 119164, 2022.

[8] Q. Hassan, M. Jaszczur, S. A. Hafedh et al., "Optimizing a microgrid photovoltaic-fuel cell energy system at the highest renewable fraction," *International Journal of Hydrogen Energy*, vol. 47, no. 28, pp. 13710–13731, 2022.

[9] H. Armghan, M. Yang, N. Ali, A. Armghan, and A. Alanazi, "Quick reaching law based global terminal sliding mode control for wind/hydrogen/battery DC microgrid," *Applied Energy*, vol. 316, article 119050, 2022.

[10] L. Tightiz, H. Yang, and A. Addeh, "An intelligent system based on optimized ANFIS and association rules for power transformer fault diagnosis," *ISA Transactions*, vol. 103, pp. 63–74, 2020.

[11] A. Singhal, V. Thanh Long, and D. Wei, “Consensus control for coordinating grid-forming and grid-following inverters in microgrids,” *IEEE Transactions on Smart Grid*, vol. 13, no. 5, pp. 4123–4133, 2022.

[12] M. Zand, M. A. Nasab, M. Khoobani, A. Jahangiri, S. H. Hosseinian, and A. H. Kimiai, “Robust speed control for induction motor drives using STSM control,” in *2021 12th Power Electronics, Drive Systems, and Technologies Conference (PEDSTC)*, Tabriz, Iran, 2021.

[13] M. A. Hanif and M. S. Bhaskar, “Spider community optimization algorithm to determine UPFC optimal size and location for improve dynamic stability,” in *2021 IEEE 12th Energy Conversion Congress & Exposition - Asia (ECCE-Asia)*, Singapore, 2021.

[14] M. Azimi Nasab, M. Zand, M. Eskandari, P. Sanjeevikumar, and P. Siano, “Optimal planning of electrical appliance of residential units in a smart home network using cloud services,” *Smart Cities*, vol. 4, no. 3, pp. 1173–1195, 2021.

[15] M. A. Nasab, M. Zand, S. Padmanaban, M. S. Bhaskar, and J. M. Guerrero, “An efficient, robust optimization model for the unit commitment considering renewable uncertainty and pumped-storage hydropower,” *Computers and Electrical Engineering*, vol. 100, article 107846, 2022.

[16] M. Azimi Nasab, M. Zand, S. Padmanaban, and B. Khan, “Simultaneous long-term planning of flexible electric vehicle photovoltaic charging stations in terms of load response and technical and economic indicators,” *World Electric Vehicle Journal*, vol. 12, no. 4, p. 190, 2021.

[17] H. Saadatinezhad, A. Ramezani, M. Alizadeh, and E. Hajimalek, “Fault tolerant load frequency sharing of a multi-area power system using model predictive control,” *The Journal of Engineering*, vol. 2022, no. 3, pp. 337–347, 2022.

[18] S. M. Ghazali, M. Alizadeh, J. Mazloum, and Y. Baleghi, “Modified binary salp swarm algorithm in EEG signal classification for epilepsy seizure detection,” *Biomedical Signal Processing and Control*, vol. 78, article 103858, 2022.

[19] S. A. Motamedi and S. Sharifian, “Multiobjective optimization in the cloud computing environment for storage service selection,” in *2018 4th Iranian Conference on Signal Processing and Intelligent Systems (ICSPIS)*, Tehran, Iran, 2018.

[20] M. Khalili and R. Hanif, “Optimal instantaneous prediction of voltage instability due to transient faults in power networks taking into account the dynamic effect of generators,” *Cogent Engineering*, vol. 9, no. 1, article 2072568, 2022.

[21] A. H. K. Asadi, A. Jahangiri, M. Eskandari, and H. Meyar-Naimi, “Optimal design of high density HTS-SMES step-shaped cross-sectional solenoid to mechanical stress reduction,” in *2022 International Conference on Protection and Automation of Power Systems (IPAPS)*, Zahedan, Iran, 2022.

[22] M. A. Nasab, M. Zand, A. Hatami, F. Nikoukar, S. Padmanaban, and A. H. Kimiai, “A hybrid scheme for fault locating for transmission lines with TCSC,” in *2022 International Conference on Protection and Automation of Power Systems (IPAPS)*, Zahedan, Iran, 2022.

[23] M. Alizadeh, S. E. Mousavi, M. T. Beheshti, and A. Ostadi, “Combination of feature selection and hybrid classifier as to network intrusion detection system adopting FA, GWO, and BAT optimizers,” in *2021 7th International Conference on Signal Processing and Intelligent Systems (ICSPIS)*, Tehran, Iran, 2021.

[24] S. Rastgoo, Z. Mahdavi, M. A. Nasab, M. Zand, and S. Padmanaban, “Using an intelligent control method for electric vehicle charging in microgrids,” *World Electric Vehicle Journal*, vol. 13, no. 12, p. 222, 2022.

[25] R. K. Dhavala and H. N. Suresh, “Effects of different batteries and dispatch strategies on performance of standalonePV/WT/DG/battery system: a case study,” *Energy Storage*, vol. 4, no. 2, article e306, 2022.

[26] M. Elkazaz, M. Sumner, S. Pholboon, R. Davies, and D. Thomas, “Performance assessment of an energy management system for a home microgrid with PV generation,” *Energies*, vol. 13, no. 13, p. 3436, 2020.

[27] F. Haroon, M. Aamir, and A. Waqar, “Second-order rotating sliding mode control with composite reaching law for two level single phase voltage source inverters,” *IEEE Access*, vol. 10, pp. 60177–60188, 2022.

[28] D. K. Jain, S. Neelakandan, T. Veeramani, S. Bhatia, and F. H. Memon, “Design of fuzzy logic based energy management and traffic predictive model for cyber physical systems,” *Computers and Electrical Engineering*, vol. 102, article 108135, 2022.

[29] H. Aziz, M. Tabrizian, M. Ansarian, and A. Ahmarinejad, “A three-stage multi-objective optimization framework for day-ahead interaction between microgrids in active distribution networks considering flexible loads and energy storage systems,” *Journal of Energy Storage*, vol. 52, article 104739, 2022.

[30] A. Jani, H. Karimi, and S. Jadid, “Multi-time scale energy management of multi-microgrid systems considering energy storage systems: a multi-objective two-stage optimization framework,” *Journal of Energy Storage*, vol. 51, article 104554, 2022.

[31] A. M. Jasim, B. H. Jasim, B. N. Alhasnawi, A. Flah, and H. Kraiem, “Coordinated control and load shifting-based demand management of a smart microgrid adopting energy internet,” *International Transactions on Electrical Energy Systems*, vol. 2023, Article ID 6615150, 33 pages, 2023.

[32] T. H. Yang, Y. H. Wen, C. K. Chiu et al., “A pre-charge tracking technique in the 40 MHz high-speed switching 48-to-5 V GaN-based DC-DC buck converter for reducing large self-commutation loss and achieving a high efficiency of 95.4%,” *IEEE Journal of Solid-State Circuits*, vol. 57, no. 7, pp. 2045–2053, 2022.

[33] X. Sun, J. Qiu, Y. Tao, Y. Ma, and J. Zhao, “A multi-mode data-driven Volt/Var control strategy with conservation voltage reduction in active distribution networks,” *IEEE Transactions on Sustainable Energy*, vol. 13, no. 2, pp. 1073–1085, 2022.

[34] K. Lu, Z. Liu, Y. Wang, C. P. Chen, and Y. Zhang, “Adaptive neural design of consensus controllers for nonlinear multiagent systems under switching topologies,” *IEEE Transactions on Systems, Man, and Cybernetics: Systems*, vol. 53, no. 1, pp. 309–320, 2023.

[35] H. Kang, S. Jung, M. Lee, and T. Hong, “How to better share energy towards a carbon-neutral city? A review on application strategies of battery energy storage system in city,” *Renewable and Sustainable Energy Reviews*, vol. 157, article 112113, 2022.

[36] A. Golshani and A. Ramezanzad, “Estimation of tensile strength for granitic rocks by using discrete element approach,” *International Journal of Geotechnical and Geological Engineering*, vol. 13, no. 8, pp. 553–557, 2019.

[37] S. F. Zandrazavi, C. P. Guzman, A. T. Pozos, J. Quiros-Tortos, and J. F. Franco, “Stochastic multi-objective optimal energy management of grid-connected unbalanced microgrids with renewable energy generation and plug-in electric vehicles,” *Energy*, vol. 241, article 122884, 2022.

[38] B. Singh and P. K. Dubey, “Distributed power generation planning for distribution networks using electric vehicles: systematic attention to challenges and opportunities,” *Journal of Energy Storage*, vol. 48, article 104030, 2022.